sustainability

MDPI

Article

Study on the Microclimatic Effects of Plant-Enclosure Conditions and Water–Green Space Ratio on Urban Waterfront Spaces in Summer

Han Xu [1,†], Guorui Zheng [2,†], Xinya Lin [3] and Yunfeng Jin [1,*]

[1] Department of Landscape Architecture, School of Architecture and Urban Planning, Tongji University, Shanghai 200092, China; 2310343@tongji.edu.cn
[2] Department of Landscape Architecture, College of Landscape Architecture and Art, Fujian Agriculture and Forestry University, Fuzhou 35002, China; 1221775053@fafu.edu.cn
[3] Longyan Agricultural School, Longyan 364000, China; 1201775025@fafu.edu.cn
* Correspondence: jinyf79@tongji.edu.cn
† These authors contributed equally to this work.

Abstract: In the context of waterfront-space design, this study examines the impact of plant enclosures and the ratio of water bodies to green spaces on the microclimate, aiming to enhance the climate environment and mitigate urban heat. Utilizing Fujian Agriculture and Forestry University as a case study, the research selects the summer solstice as a representative weather condition, conducts field measurements and model validation for four types of waterfront vegetation, and creates 80 scenarios with varying plant enclosures and water to green space ratios using ENVI-met 5.0.2software. This comprehensive analysis seeks to identify the optimal water–green space ratio for waterfront areas. Key findings include: (1) The efficacy and applicability of ENVI-met software for microclimate studies are confirmed. (2) Waterfront plants have cooling and humidifying effects on the microclimate environment. The order of cooling and humidifying effects of different plant community structures was as follows: tree–shrub–grass > tree–grass > shrub–grass > grass. (3) The cooling, humidification, ventilation, and human comfort levels are influenced by the specific enclosure conditions and water to green space ratios; a ratio of 1.8:1 is the most effective for cooling and improving human comfort, while ratios of 4:1 and 1:4 are better for humidification and ventilation. These results offer valuable insights for designing waterfront spaces in hot and humid climates.

Keywords: summer; plants; enclosure conditions; water body–green space ratio; urban waterfront space; microclimate effects

check for updates

Citation: Xu, H.; Zheng, G.; Lin, X.; Jin, Y. Study on the Microclimatic Effects of Plant-Enclosure Conditions and Water–Green Space Ratio on Urban Waterfront Spaces in Summer. *Sustainability* **2024**, *16*, 2957. https://doi.org/10.3390/su16072957

Academic Editor: Georgios Koubouris

Received: 23 February 2024
Revised: 29 March 2024
Accepted: 29 March 2024
Published: 2 April 2024

Copyright: © 2024 by the authors. Licensee MDPI, Basel, Switzerland. This article is an open access article distributed under the terms and conditions of the Creative Commons Attribution (CC BY) license (https://creativecommons.org/licenses/by/4.0/).

1. Introduction

The urban ecological environment is currently under significant stress due to challenges such as global warming and extreme heat, which pose severe threats to city dwellers' physical and mental health [1]. As critical components of the urban ecosystem, waterfront spaces play a pivotal role in enhancing the environmental microclimate and the comfort of inhabitants. Consequently, investigating the effects of the microclimate on urban waterfront spaces is paramount [2,3].

It has been shown that the blue–green characteristics of waterfront spaces (water bodies and plant greenery) are the main factors influencing the microclimate [4]. On the one hand, water bodies and plant greenery will have different degrees of influence on the surrounding environment due to their own physical properties. Firstly, water bodies have the characteristics of large heat capacity, large latent heat of evaporation, and small water surface reflectivity, which can absorb and store a large amount of heat, and can be used as an urban cooling source, which is conducive to alleviating the heat island effect over and near the water bodies [5,6]. Secondly, plant greening can not only form a

shade layer by directly blocking solar radiation through the tall canopy crown; it can also reduce the surrounding temperature through the pathway of evapotranspiration. Usually, after absorbing most of the solar radiation, trees convert sensible heat into latent heat and vaporize water to absorb heat [7], thus increasing the humidity of the surrounding air [8], lowering the ambient temperature, and improving the urban thermal environment and thermal comfort [9]. On the other hand, the enclosure conditions of plants and the water–green space ratio are closely related to the microclimate effect. Related studies have shown that different plant-enclosure conditions can produce different microclimatic effects. Fung et al. studied the microclimatic effects of plant greening on waterfront space in summer, and the results showed that water bodies shaded by trees have more beneficial effects on the thermal environment of the grassland than those not shaded by trees [10]. On this basis, Lin et al. and Song et al. tried to explore the combination of plant greening in different waterfront spaces; tall and highly depressed trees can be planted in the waterfront walkway space, and trees and grass can be combined in the waterfront recreation space [11], to improve the ventilation environment, increase the shaded area, and reduce the surrounding environmental temperature [12]. In addition, different water body to green space ratios also produce different microclimate effects. Mirela Robitu et al. found through microclimate assessment of cities that the combination of river water bodies and plant greenery can significantly reduce the summer surface temperature and improve comfort [13]; Li Kongqing et al. found that the strength of the role of water body-microclimate-regulating properties will be affected by the external space and vegetation [14]. Xu et al. concluded that the microclimatic effect of the campus plaza is related to the water body footprint and that the microclimatic effect stays the same when the water body footprint exceeds 36% of the area [15]. The current research on the microclimate of waterfront space focuses on the improvement of the urban thermal environment [16] and comfort [17] by spatial features [18], plant communities [19,20], and water body layout [21] and lacks a systematic research study on the microclimate effect of different blue–green features on waterfront space. Therefore, it is necessary to discuss the effects of various water body–green space ratios on microclimate under different enclosure conditions to provide a theoretical basis and data reference for the improvement of the microclimate environment in waterfront spaces and to enrich the research knowledge of urban microclimates.

Actually, in the urban construction landscape, the area of green space and water bodies that can be used for planning and layout is limited. Therefore, we need to carry out a multi-physical quantity and multi-probability simulation process through numerical simulations to improve efficiency, save costs, and choose the best simulation method for implementation. Studies have shown [22,23] that ENVI-met can realize parametric control of many environmental conditions, has high accuracy and sensitivity, can reflect the actual situation well, and has been widely used in climate environment simulation [24,25]. For example, Zhang et al. took Wuhan as an example, simulated the impact of different vegetation scenarios on the thermal environment with the help of ENVI-met, and finally chose the best plant configuration [26]. Xu et al. took campus green space as the research object and explored the best green space optimization scheme design based on ENVI-met numerical simulation [27]. Therefore, we will utilize this software fully to systematically analyze the microclimate effect of waterfront space with different plant-enclosure conditions and water–green space occupancy ratio.

Based on this aim, this study focuses on Fujian Agriculture and Forestry University as the case study area, assessing the microclimate parameters across four plant community configurations. Utilizing ENVI-met, it models 80 different scenarios to investigate the effects of plant enclosures and water to green space ratios on the microclimate. The findings culminate in identifying the optimal microclimate regulation configuration. This model offers valuable insights for improving the design of waterfront spaces during summer.

2. Materials and Methods

2.1. Study Area

The area selected for this study was Fujian Agriculture and Forestry University (Qishan Campus). Fujian Agriculture and Forestry University (Qishan Campus) is located in Fuzhou City, which is in the eastern part of Fujian Province, in the lower reaches of the Minjiang River and the coastal area (26°04′27″ N, 119°17′47″ E), with a typical subtropical monsoon climate and an average annual humidity of 74%. It is a typical subtropical monsoon climate with an average annual humidity of 74%. The summer is characterized by persistent high temperatures, with the highest temperature as high as 40 °C, which has been regarded as one of China's "four great furnaces". The reasons for selecting this campus as the research object include the following: (1) Fujian Agriculture and Forestry University (Qishan Campus) is a university campus under construction, and the study results are expected to be applied to practice. (2) The campus accommodates more than 20,000 students and teachers, and the waterfront space carries the essential functions of leisure, recreation, and study for the students and teachers. High temperatures and hot and humid environments directly affect the feelings of the students and teachers and the frequency of use of spaces, and the task of alleviating the high thermal environment of the waterfront space is very urgent. (3) The plant community in the waterfront space covers the plant community in the hot and humid area, which is rich in number, numerous in species, stable in growth, well managed, and suitable for this study. (4) The waterfront space on campus has complete blue–green landscape elements, and the study of its waterfront space is conducive to its extension to a larger area, providing a reference for the future design of other types of waterfront space (Figure 1).

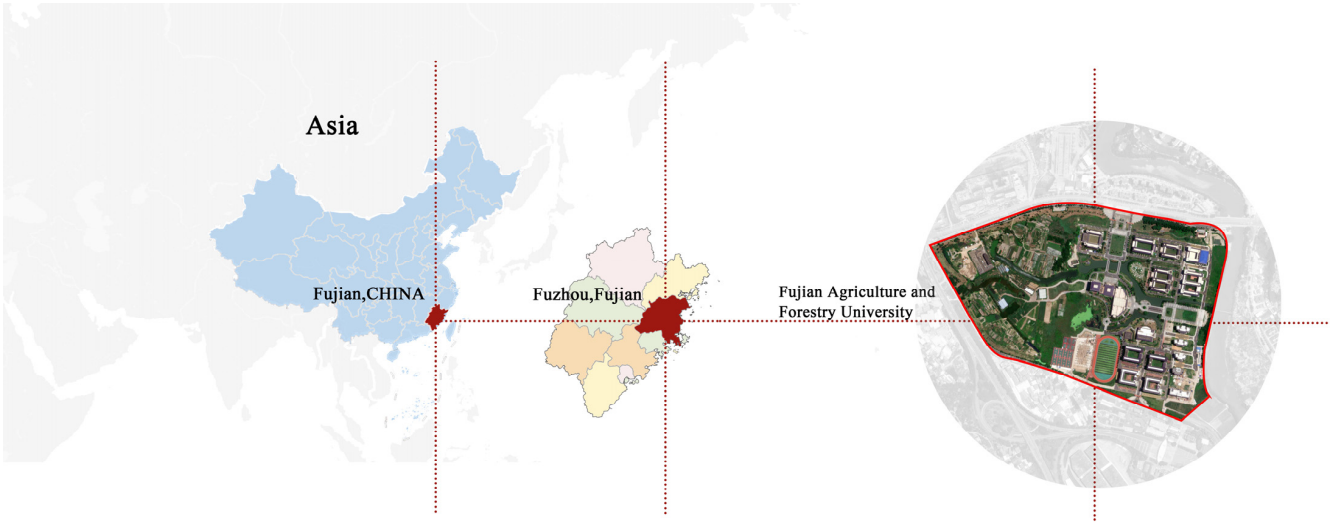


Figure 1. Study area.

2.2. Field Measurement

In this paper, the summer solstice was selected for field measurements. The summer solstice usually occurs on 21 June in the northern hemisphere. It represents the day with the longest sunshine hours [28], with distinct microclimatic characteristics (temperature, humidity, wind speed), and it is also considered to be the warmest day of the year in China [29]. This period is crucial for studying the microclimatic effects of vegetation and water bodies to effectively mitigate the urban heat island effect. Meanwhile, selecting a typical summer solstice for climate and comfort assessment has ensured that the study results are robust and valid under the widest possible range of conditions [30].

A Kestrel 5500 Meteorometer (accuracy ±0.5 °C, ±2.5%RH, ±0.1 m/s; range −29~70 °C, 0~100%RH, 0~40 m/s) was used to determine the air temperature (°C), relative humidity (%) and wind speed (m/s). The field measurements were selected on summer 2022.06.21

(summer solstice), under smooth airflow and clear weather conditions, to determine the microclimates of four different plant community structures. The current water body–green space ratio of the waterfront space was 1:1.8, and in order to improve the accuracy of the measurements, four different measurement points were selected for each plant community (Figure 2), and the measured data were taken as the average of the four points. At the same time, a control point was set at the place without plant community coverage. In total, there were 16 measurement points and one control point, and the measurement points are shown in Table 1. The test time was from 8:00 to 18:00. In the experiment, the meteorological instruments were placed to allow use of the manual movement detection method for the 16 sample plots and hand-held measuring instruments were used to measure and record the detailed data. Then, these were quickly rushed to the next measurement point, and the interval time for switching the measurement points was as similar as possible, with an interval of 1 h, and the results were recorded as an average value. The measured data were used to analyze the daily trends (temperature, humidity, and wind speed) in waterfront spaces created with different plant community-planting methods, and they were used to verify the model accuracy of ENVI-met.

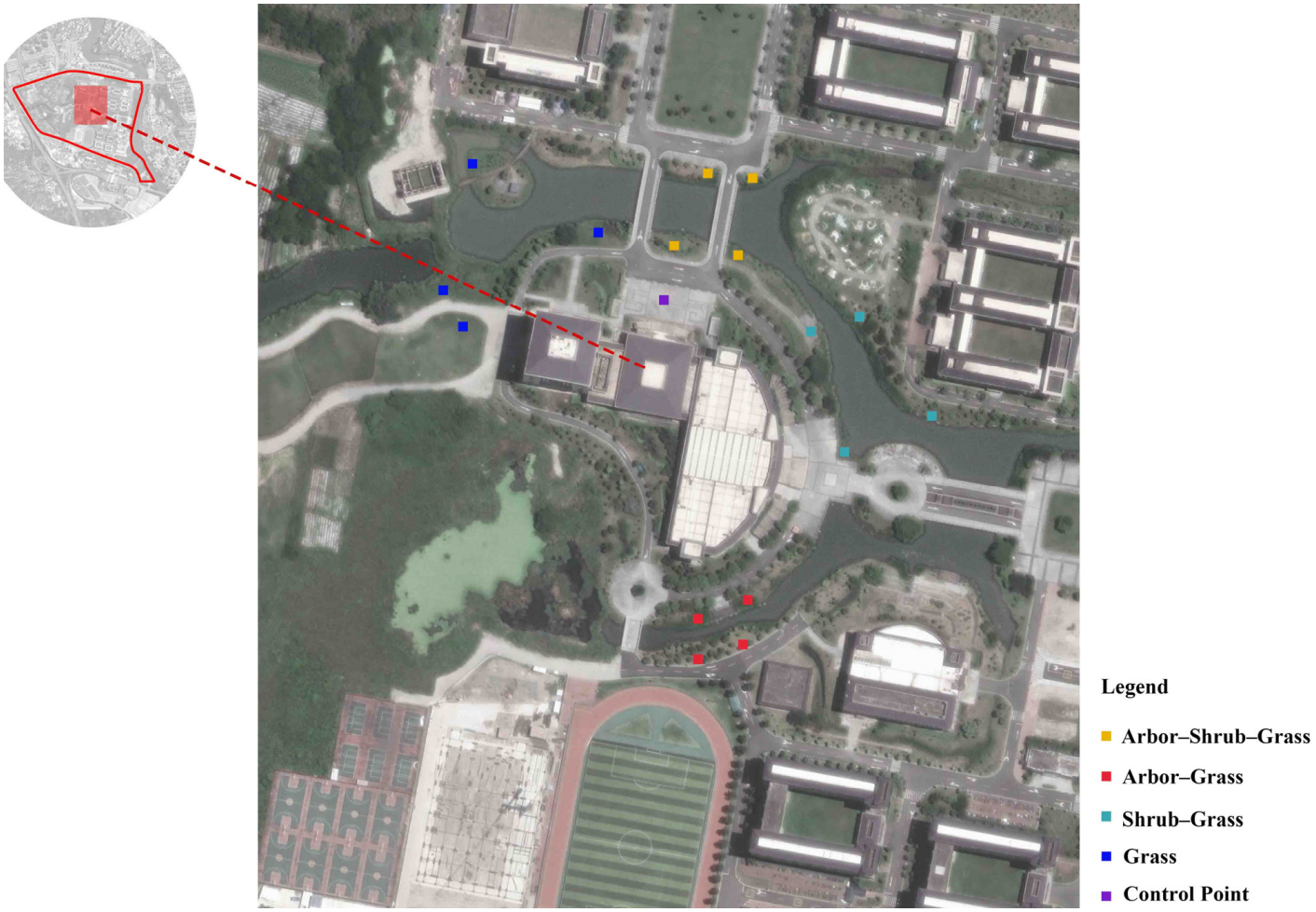


Figure 2. Distribution of measurement points in waterfront spaces.

Table 1. Overview of measurement points.

Measurement Point Type and Identification	Plant Community Type	Spatial Characteristic	Photographs of Measurement Point
1	Grass	The perimeter is open and the ground cover plants area dominated by *Zoysia matrella*.	
2	Shrub–grass	Enclosed by shrubs. Shrubs are mainly *Nerium oleander* and *Cyperus involucratus*. Ground cover plants were mainly *Zoysia japonica*.	
3	Tree–grass	Enclosed by trees. The ground cover is *Ophiopogon bodinieri*. Trees are *Camphora officinarum*.	
4	Tree–shrub–grass	Enclosed by trees. Trees are mainly *Bischofia javanica*, *Melaleuca bracteata*, *Liriodendron chinense*. Shrubs are mainly *Hibiscus rosa-sinensis*, *Fagraea ceilanica*, *Cordyline fruticosa*, *Bougainvillea spectabilis*. Ground covers are *Zoysia japonica*.	
Control point		Open space. Hard paved floors	

2.3. ENVI-Met Simulation

2.3.1. Model Validation

Meteorological data were obtained by logging into the Chinese weather website (https://rp5.ru/) on 21 June 2022, which provided initial meteorological data for the ENVI-met simulation parameter settings. According to the physical size of the site, the ENVI-met modeling grid size is 270 m × 180 m × 30 m. The grid cell size is set as dx = 4, dy = 4, dz = 3. The simulation time is from 5:00–19:00, and the data from 8:00–18:00 are selected for the study. In order to ensure that the simulation is consistent with the measured environmental conditions, the initial parameters of the model simulation, such as plot size, meteorological

parameters, surrounding environment, vegetation status, and time, are set to be consistent with the parameters of the measured waterfront space. Details of other parameter settings are shown in Table 2.

Table 2. Model validation parameter settings.

Parameter Name	Parameter Name	Parameter Values
Grid settings	Model dimensions/size of grid cell in meter	270 × 180 × 30/4 m × 4 m × 3 m
Model location	Base settings	Fujian Agriculture and Forestry University (Qishan Campus). 26.08° N, 119.23° E
	Microscale roughness length of surface (m)	0.01
Time and date	Start date	21 June 2022
	Start time	5:00 a.m.
	Total simulation time	14
Meteorological data	Specific humidity in 2500 m (g/kg)	7
	Wind direction	135° (south-east)
	Windspeed (m/s)	2.5
	Temperature range	17–28
Soil section	Upper layer (0–20 cm)	65 °C/50%RH
	Middle layer (20–50 cm)	70 °C/50%RH
	Deep layer (50–200 cm)	75 °C/50%RH

2.3.2. Modeling Scheme

In this study, we used the planting of trees as a condition of enclosure of the waterfront space. According to the tree height, morphology, and leaf area index of 100 common trees in Fuzhou City, we set the simulated tree species with a tree height of 10 m, umbrella-like morphology, and leaf area index of 3.95 [31]. According to the research results of the previous researchers [32], the green space of waterfront space should account for 35%~75% of the total area of waterfront; the optimal ratio of trees, shrubs, and grasses in the green space of waterfront is 2:2:1; and the height of closed spaces should not be more than 1/2 of the width of the site.

Based on the above requirements, ENVI-met software was used to establish a three-dimensional model with a model size of 40 m×40 m×10 m and grid cell sizes of dx = 1, dy = 1, and dz = 3; the maximum height of the trees in the model was 10 m; the proportion of the water area to the total area was set to be 80%, 65%, 50%, 35%, and 20% and the ratios of the green space to the hard pavement were 1:4 (I), 1:1.8 (II), 1:1 (III), 1.8:1 (IV), 4:1 (V); the enclosure conditions are set as open (A), semi-open [one side of an enclosure] (B), [two sides of an enclosure] (C), [three sides of an enclosure] (D), and full enclosure (E)] (Appendix A).

2.4. Data Analysis

First, we used software such as SPSS 13.0 and SigmaPlot 14.0 to calculate Root Mean Square Error (RMSE), Mean Absolute Error (MAE), and Mean Absolute Percentage Error (MAPE) to measure the observed and simulated values of the deviation and evaluate the accuracy of the model [33] (Equations (1)–(3)) and to quantitatively analyze the correlations between enclosure, water body–green space ratio, and microclimate and human comfort improvement index. Secondly, for the climatic conditions of Fuzhou City, the three elements of air temperature, relative humidity, and wind speed were selected as the primary evaluation indexes to calculate the human comfort improvement index [34] (Equation (4)) under the influence of enclosure conditions and water body–green space ratio. The evaluation of the comfort index was based on the 9-level standard division method published by the China Meteorological Administration, in which the application range of human comfort in the humid and hot zone in summer was 6 to 9 levels. Finally, the changes in cooling index, humidification index, ventilation index, and comfort improvement index were used to

reflect the strength of the microclimate regulation effect of enclosure conditions and water body–green space ratio on waterfront space [35] (Equations (5)–(8)) (Table 3).

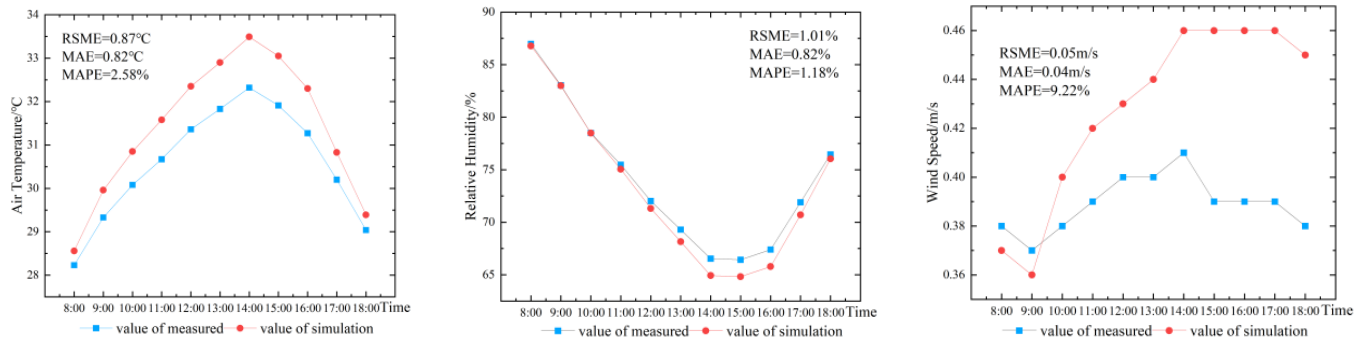
Table 3. Data calculation formula.

Equation Number	Formula	Meaning	Symbol and Its Representation	Reference
(1)	$RMSE = \sqrt{\frac{\sum_{i=1}^{n}(x_i - x_i')^2}{n}}$	Evaluate the accuracy of the model, compare the error between the measured and simulated values, and reflect the applicability of the model.	x_i denotes the simulated value x_i' denotes the measured value n denotes the number of tests	[34]
(2)	$MAE = \frac{1}{n}\sum\lvert x_i - x_i'\rvert$			
(3)	$MAPE = \frac{1}{n}\sum_{i=1}^{n}\frac{\lvert x_i - x_i'\rvert}{xi} \times 100\%$			
(4)	$Ci = 1.8Ta + 0.55(1 - Rh)32 + 32\sqrt{Va}$	Evaluate the level of human comfort in different meteorological conditions.	Level 6: 65–70 (warm, comfortable). Level 7: 70–75 (hot, more comfortable). Level 8: 75–80 (stuffy, uncomfortable). Level 9: >80 (Extremely stuffy, extremely uncomfortable).	[35]
(5)	$\Delta Ta = \frac{Tam - Tac}{Tac} \times 100\%$	The cooling index, humidification index, ventilation index, and comfort improvement index were used to indicate the improvement extent of the plaza's microclimate and of human comfort.	ΔTac, ΔRhc, ΔVac, ΔCic, ΔTam, ΔRhm, ΔVam, and ΔCim denote, respectively, the air temperature, relative humidity, wind speed, comfort index of the control point and the measurement point	[36,37]
(6)	$\Delta RH = \frac{Rhm - Rhc}{Rhc} \times 100\%$			
(7)	$\Delta Va = \frac{Vam - Vac}{Vac} \times 100\%$			
(8)	$\Delta Ci = \frac{Cic - Cim}{Cic} \times 100\%$			

3. Results

3.1. Comparative Analysis of the Errors between Simulated and Measured Value

By comparing the average measured and simulated values of microclimate elements in summer in the waterfront space (Figure 3), it can be seen that the fluctuation trends of the simulated and measured results are consistent with a high degree of fit; the error between the daily average simulated temperature and the measured temperature is 0.33 °C~1.18 °C; the error between the daily average simulated humidity and the measured humidity is 0.03%~1.62%; the error between the daily average simulated wind speed and the measured wind speed is less than 0.5 m/s. The RMSE values between the simulated and measured temperature, humidity, and wind speed values in the study area are 0.87 °C, 1.01% and 0.5 m/s, respectively; the MAE values were 0.82 °C, 0.82%, and 1.18 m/s, respectively; and the MAPE values were 2.58%, 1.18%, and 9.22%, respectively. The reasonable error ranges of the model are RMSE: 0~1.5, MAE: 0~1.5, and MAPE $\leq$ 10%, which indicates that the model is highly accurate and the experimental results are valid.

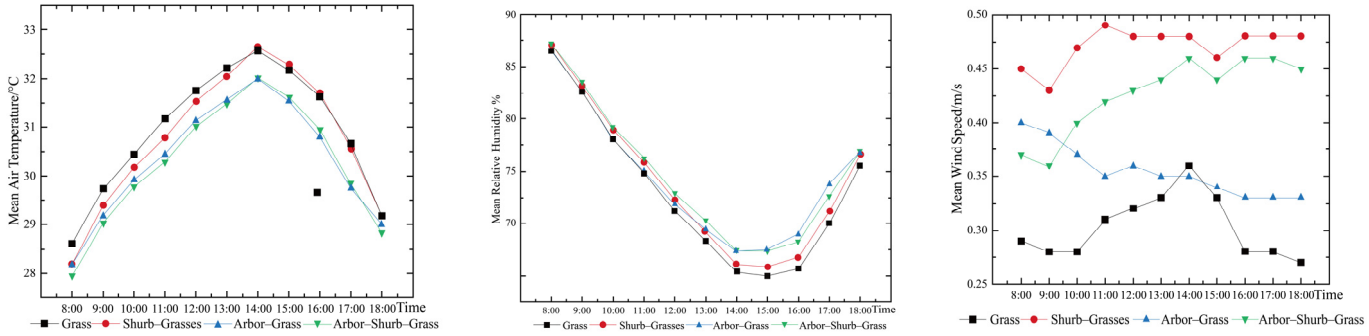


(**a**) (**b**) (**c**)

Figure 3. Fitting diagrams of the simulated and measured values of summer microclimate factors at the measurement points. (**a**) Temperature; (**b**) Humidity; (**c**) Wind speed.

3.2. Analysis of Measured Results of Plant Communities in Waterfront Spaces

Four kinds of plant community structures in the waterfront space, namely grass, arborvitae, shrub–grass, and arborvitae, were selected as research objects, and the average values of temperature, humidity, and wind speed were counted and the daily trends were analyzed in each test period in summer in the humid and hot zone (Figure 4).



(**a**) (**b**) (**c**)

Figure 4. Fitting diagram of the simulated and measured values of summer microclimate factors at the measurement points. (**a**) Temperature; (**b**) Humidity; (**c**) Wind speed.

(1) Temperature. The average daily temperatures of different plant communities in waterfront spaces in summer had the same trend. The overall trend was an inverted U-shaped curve which increased and then decreased. All the maximum temperatures occurred at 14:00 p.m. and the minimum temperatures occurred at 8:00 a.m. The temperature of grassland varied from 28.64 °C to 32.57 °C with a mean daily temperature of 30.92 °C. At 14:00 p.m., the lowest air temperature was 27.94 °C for tree–shrub–grass, followed by the tree–grass and shrub–grass plant communities with temperatures of 31.13 °C and 31.54 °C, the highest air temperature was 31.76 °C for grass. At 8:00 a.m., the order in terms of coolness of the plant community was: tree–shrub–grass (coolest) > tree–grass > shrub–grass > grass, and the air temperatures were: 27.94 °C, 28.17 °C, 28.18 °C, and 28.61 °C, respectively.

(2) Humidity. The daily average humidity of different plant communities in waterfront spaces in summer had the same trend. The overall trend showed a U-shaped curve which decreased and then increased, with the lowest humidity occurring at 15:00 p.m. and the highest humidity occurring at 8:00 a.m. The humidity of the tree–shrub–grass varied from 67.30% to 87.18%, and the daily average humidity was 74.71%. Compared to tree–shrub–grass, grassland had the lowest average daily humidity of 73.01%, followed by tree–grass at 74.39%. At 15:00 p.m., tree–grass had the highest relative humidity of 67.51%, followed by tree–shrub–grass and shrub–grass plant communities at 67.30% and 65.89%, respectively, and grass had the lowest relative humidity of 65.03%. At 8:00 a.m., the order of highest humidity in the plant community was: tree–shrub–grass > tree–grass > shrub–grass > grass, and the relative humidity was: 87.18%, 87.08%, 87.07%, and 86.54%, respectively.

(3) Wind speed. The wind speed fluctuated in summer at each measurement point. The shrub–grass had the highest average wind speed and the best ventilation. (wind speeds ranged from 0.47 to 0.48 m/s, with an average wind speed of 0.47 m/s), followed by tree–shrub–grass (wind speeds ranged from 0.36 to 0.46 m/s, with an average wind speed of 0.43 m/s) and shrub–grass (wind speeds ranged from 0.32 to 0.39 m/s, with an average wind speed of 0.35 m/s). Grassland had the worst ventilation (wind speed range from 0.27 to 0.36 m/s, mean wind speed of 0.30 m/s).

3.3. Analysis of the Effects of Different Enclosure Conditions and Water–Green Space Ratio on Microclimate and Comfort Level

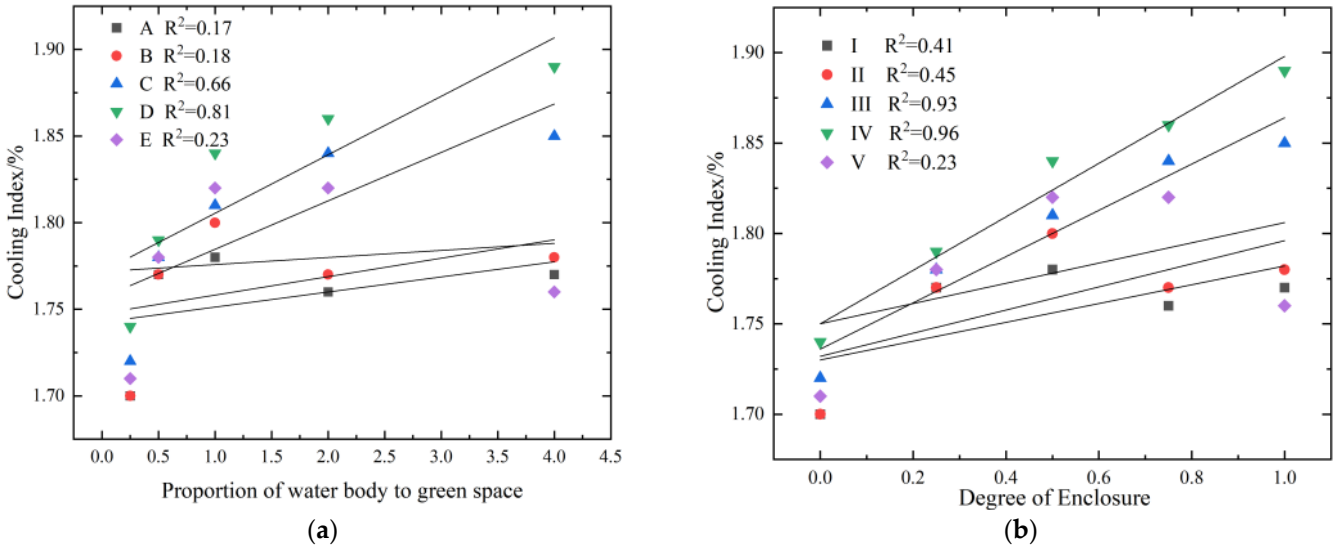
(1) Cooling index. Comparative calculation of the average summer cooling index (Table 4) found that, under the same enclosure conditions, different water body–green space ratios have different effects on temperature regulation. With the increase in water body percentage, the cooling index showed a trend of increasing and then decreasing. Comparing the average value of each water body–green space ratio, it can be seen that the water body–green space ratio of 1.8:1 has the best heat preservation effect, with an average cooling index of 1.83 °C, followed by the water body–green space ratios of 4:1 and 1:1, with an average cooling index of 1.80 °C. By analyzing the correlation between the water body–green space ratio and the cooling index (Figure 5a), it was found that the water body–green space ratio was significantly positively correlated with the cooling index under the three-side enclosure space (R^2 = 0.81), and the water body–green space ratio was positively correlated with the cooling index under the two-side enclosure space (R^2 = 0.66), i.e., the three-side enclosure space > two-side enclosure space. In all other enclosure conditions, the correlation was not significant. By analyzing the correlation between the enclosure and the cooling index (Figure 5b), it was found that the spatial enclosure cooling and the temperature index were significantly positively correlated (R^2 = 0.96) when the water body–green space ratio was 1.8:1 and that the spatial enclosure was significantly positively correlated with the cooling index when the water body–green space ratio was 1:1 (R^2 = 0.93), i.e., the water body–green space ratio of 1.8:1 > the water body–green space ratio of 1:1. The other enclosures were not strongly correlated with the cooling index. A comprehensive comparison shows that the average cooling benefit of B4 (enclosure on the east side) is better. The cooling index is the highest at 2.03% for a water body–green space ratio of 1.8:1, and the cooling indices of the other water body–green space ratios are in the following order: 2.02%, 2.02%, 2.01%, and 2.00%, followed by C4 (enclosure on the southwestern side), and the space with a water body–green space ratio of 1.8:1. The cooling indices were all 1.99%.

Table 4. Waterfront-space cooling index variation under the effects of different enclosure conditions and waterbody–green space ratio.

Enclosure Condition			Water Body–Green Space Ratio				
Index	**Enclosure Degree**	**Enclosure Direction**	**I-1:4**	**II-1:1.8**	**III-1:1**	**IV-1.8:1**	**V-4:1**
Cooling index	A	-	1.70	1.70	1.72	1.74	1.71
	B	B1—North	1.59	1.60	1.60	1.60	1.60
		B2—South	1.70	1.70	1.71	1.72	1.71
		B3—West	1.75	1.77	1.79	1.82	1.80
		B4—East	2.02	2.02	2.01	2.03	2.00
	C	C1—West-North	1.67	1.67	1.67	1.68	1.66
		C2—South-North	1.76	1.76	1.78	1.82	1.80
		C3—East-North	1.78	1.78	1.82	1.85	1.82
		C4—West-South	1.89	1.90	1.91	1.99	1.94
		C5—East-West	1.79	1.88	1.88	1.89	1.88
		C6—East-South	1.78	1.78	1.78	1.82	1.81

Table 4. *Cont.*

Enclosure Condition			Water Body–Green Space Ratio				
Index	**Enclosure Degree**	**Enclosure Direction**	**I-1:4**	**II-1:1.8**	**III-1:1**	**IV-1.8:1**	**V-4:1**
Cooling index	D	D1—North-South-West	1.78	1.82	1.87	1.86	1.87
		D2—North-South-East	1.72	1.72	1.76	1.76	1.86
		D3—East-West-North	1.82	1.82	1.86	1.92	1.82
		D4—East-West-South	1.73	1.73	1.85	1.90	1.75
	E	East-South-West-North	1.77	1.78	1.85	1.89	1.76
	Average value		1.77	1.78	1.80	1.83	1.80



(**a**) (**b**)

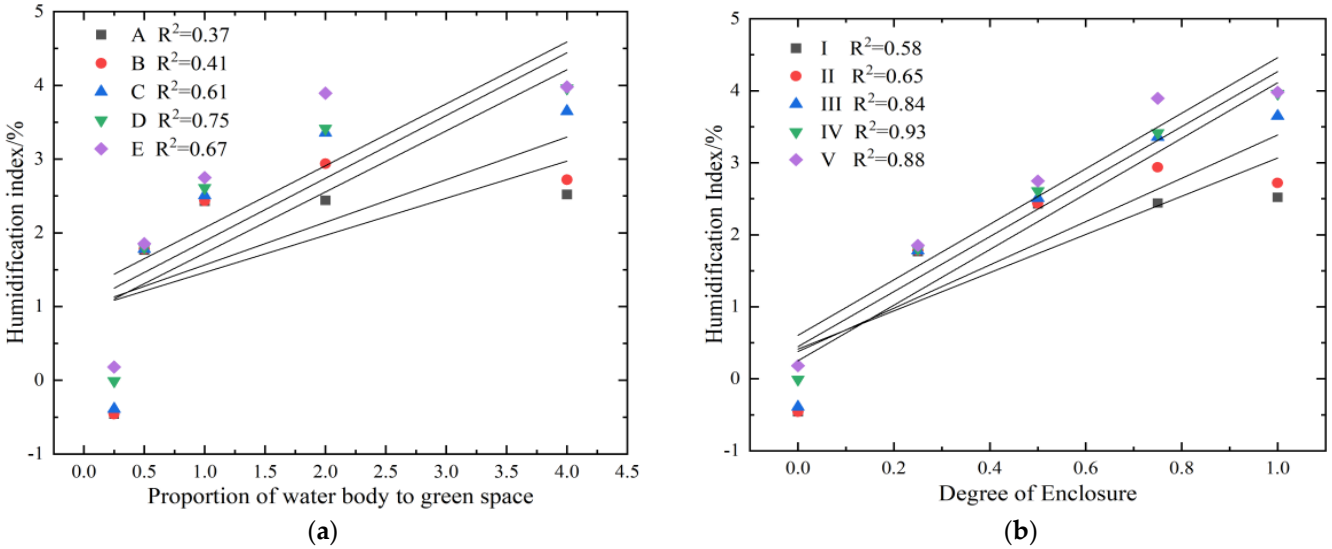
Figure 5. Correlation analysis of enclosure conditions, water body–green space ratio, and waterfront-space cooling index. (**a**) Water body–green space ratio; (**b**) Enclosure condition.

(2) Humidification index. The higher the content of water molecules in the air in summer, the better the humidification benefit and the better the improvement of the environment. From Table 5, it can be seen that under the same enclosure conditions, different water body–green space ratios have different humidification effects. The higher the water body–green space ratio, the higher the relative humidity, which is due to the presence of a large number of water molecules in the water body that can increase humidity. The average humidification rates were 2.09%, 2.23%, 2.43%, 2.53%, and 2.73% for water body–green space ratios of 1:4, 1:1.8, 1:1, 1.8:1, and 4:1, with the humidification rate increasing in that order. Analyzing the correlation between the water body–green space occupancy ratio and the humidification index, it was found (Figure 6a) that the water body–green space ratio and the humidification index were positively correlated under different enclosure conditions. Among them, the correlation between water body–green space ratio and humidification index was significantly positive under three-side enclosure, four-side enclosure, and two-side enclosure conditions (R^2 = 0.93, R^2 = 0.88, and R^2 = 0.84). Analyzing the correlation between the enclosure and the humidification index found (Figure 6b) that spatial enclosure was positively correlated with the humidification index at water body–green space ratios of 1:1, 1.8:1, and 4:1 (R^2 = 0.61, R^2 = 0.75, and R^2 = 0.67). Taken as a whole, different enclosure conditions showed different regulatory effects on humidity, and the highest humidification effect was found in D2 (three-sided enclosure in the north-south-east and south-east, with a water–green space ratio of 4:1) and D4 (three-sided enclosure in the east-west and south-west, with a water–green space ratio of 4:1), with humidifica-

tion rates of 4.88%, and 4.66%, respectively; these were followed by E, the space with water–green space ratios of 1.8:1, 4:1, which had a humidification rate of 3.96%, 3.98%.

Table 5. Waterfront-space humidification index variation under the effects of different enclosure conditions and water body–green space ratios.

Enclosure Condition			Water Body–Green Space Ratio				
Index	**Enclosure Degree**	**Enclosure Direction**	**I-1:4**	**II-1:1.8**	**III-1:1**	**IV-1.8:1**	**V-4:1**
Humidification index	A	-	−0.46	−0.46	−0.39	−0.01	0.18
	B	B1—North	1.78	1.80	1.81	1.84	1.87
		B2—South	1.78	1.80	1.81	1.83	1.87
		B3—West	1.77	1.74	1.75	1.76	1.79
		B4—East	1.75	1.80	1.81	1.82	1.86
	C	C1—West-North	2.32	2.37	2.36	2.37	1.87
		C2—South-North	2.36	2.14	2.20	2.26	2.18
		C3—East-North	2.46	2.38	2.49	2.58	2.96
		C4—West-South	2.38	2.62	2.77	2.87	2.65
		C5—East-West	2.50	2.51	2.61	2.81	2.89
		C6—East-South	2.56	2.58	2.64	2.74	3.94
	D	D1—North-South-West	2.78	2.89	2.89	2.99	3.00
		D2—North-South-East	2.18	2.90	3.74	3.76	4.88
		D3—East-West-North	2.11	2.98	3.10	3.18	3.04
		D4—East-West-South	2.68	2.97	3.69	3.76	4.66
	E	East-South-West-North	2.52	2.72	3.65	3.96	3.98
	Average value		2.09	2.23	2.43	2.53	2.73



(**a**) (**b**)

Figure 6. Correlation analysis of enclosure conditions, water body–green space ratio and waterfront-space humidification index. (**a**) Water body–green space ratio; (**b**) Enclosure condition.

(3) Ventilation index. Table 6 shows that under the same enclosure conditions, different water body–green space ratios have different effects on the regulation of wind speed. Observation of the ventilation index values revealed that the waterfront space was best ventilated when plants were not enclosed, and the water body–green space

ratio was 1:4, with an average ventilation index of 0.94%. Analyzing the correlation between water body–green space occupancy and humidification index, it was found (Figure 7a) that the water body–green space ratio was negatively correlated with the ventilation index under the same enclosure condition and that the water body–green space ratio under the no-enclosure space had a significant negative correlation with the ventilation index (R^2 = 0.99). As shown in Figure 7b, the degree of enclosure was negatively correlated with the ventilation index, where the strongest correlation was for the waterfront space with a waterbody–green space ratio of 1:4 (R^2 = −0.97). Enclosure degree, enclosure direction, and underlayment ratio each had an effect on wind speed. In summary, A (unobstructed), with a waterbody–green space ratio of 1:4, had the best ventilation index of 1.55%. This was followed by B3 (enclosure on the west side, enclosure on the south side, enclosure on the east side, and enclosure on the north side) with a water body–green space ratio of 1:4, with ventilation indices of 1.41%, 1.30%, 1.24%, and 1.09%, respectively.

Table 6. Waterfront-space ventilation index variation under the effects of different enclosure conditions and waterbody–green space ratios.

Enclosure Condition			Water Body–Green Space Ratio				
Index	**Enclosure Degree**	**Enclosure Direction**	**I-1:4**	**II-1:1.8**	**III-1:1**	**IV-1.8:1**	**V-4:1**
Ventilation index	A	-	1.55	0.56	0.56	0.57	0.54
	B	B1—North	1.09	0.38	0.38	0.38	0.25
		B2—South	1.30	0.38	0.39	0.33	0.11
		B3—West	1.41	0.35	0.36	0.35	0.13
		B4—East	1.24	0.40	0.42	0.31	0.16
	C	C1—West-North	0.98	0.43	0.43	0.43	0.26
		C2—South-North	0.85	0.40	0.40	0.41	0.23
		C3—East-North	0.88	0.36	0.36	0.36	0.19
		C4—West-South	0.91	0.34	0.34	0.35	0.11
		C5—East-West	0.93	0.42	0.42	0.42	0.27
		C6—East-South	0.91	0.39	0.39	0.39	0.20
	D	D1—North-South-West	0.68	0.46	0.46	0.47	0.45
		D2—North-South-East	0.64	0.42	0.43	0.43	0.43
		D3—East-West-North	0.66	0.44	0.44	0.45	0.40
		D4—East-West-South	0.66	0.44	0.44	0.45	0.41
	E	East-South-West-North	0.28	0.24	0.25	0.25	0.25
	Average value		0.94	0.40	0.40	0.40	0.27

(4) Human comfort index. As shown in Table 7, the degree of enclosure, the direction of enclosure, and the water–green space ratio improved human comfort to some extent. As shown in Figure 8a, different water body–green space ratios under the same enclosure conditions had different improvement effects on the comfort index. The water–green space ratio under the two-side enclosure space was negatively correlated with the comfort improvement index; the water–green space ratio under the entire enclosure space was significantly positively correlated with the comfort improvement index; and there was no significant correlation between the water–green space ratio and the comfort improvement index under the rest of the enclosure conditions. Comparing the average comfort improvement indexes of water–green space ratios, it was found that the most extensive average comfort improvement index was 15.99%

for a water–green space ratio of 1.8:1, and the smallest average comfort improvement index was 15.36% for a water–green space ratio of 4:1. Under the condition of the same water body–green space ratio, different enclosure degrees and enclosure directions have different abilities to improve the human comfort index. When the water body–green space ratio was 1:1, the degree of enclosure was negatively correlated with the comfort improvement index; when the water body–green space ratio was 4:1, the degree of enclosure was significantly positively correlated with the comfort improvement index, and the rest were not significantly correlated (Figure 8b). Taken together, the most significant improvement index was C4 (two southwestern enclosures, water–green space ratio of 1:4) at 17.38%, followed by C3 (two northeastern enclosures, water–green space ratio of 1:4) at 17.34%, and then C4 (two southwestern enclosures, water–green space ratio of 1.8:1), all with an improvement index of 17.27%.

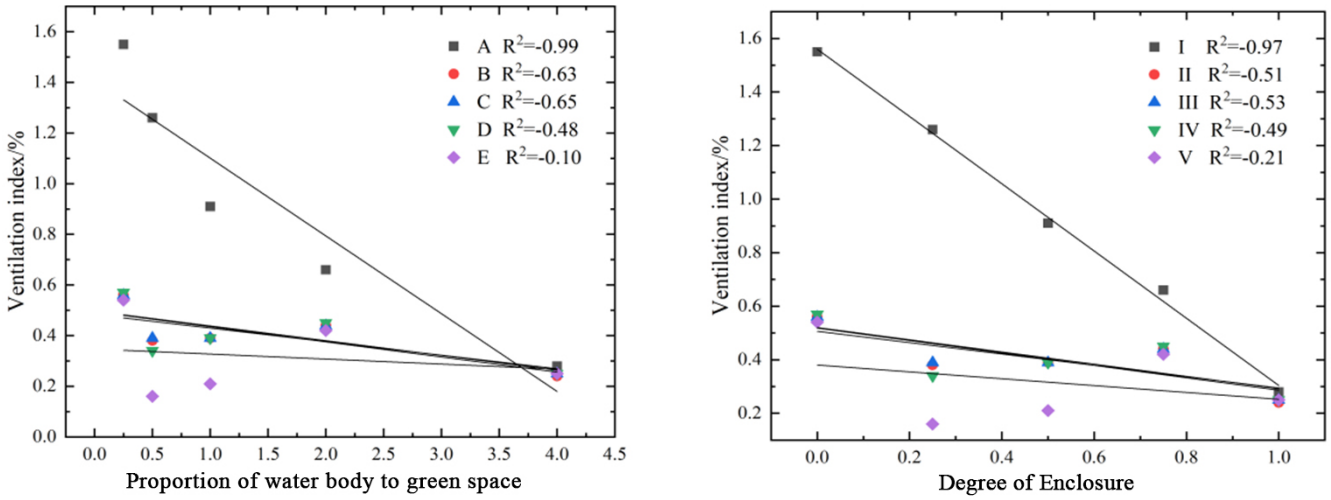


Figure 7. Correlation analysis of enclosure conditions, water body–green space ratio, and waterfront-space ventilation index. (**a**) Water body–green space ratio; (**b**) Enclosure condition.

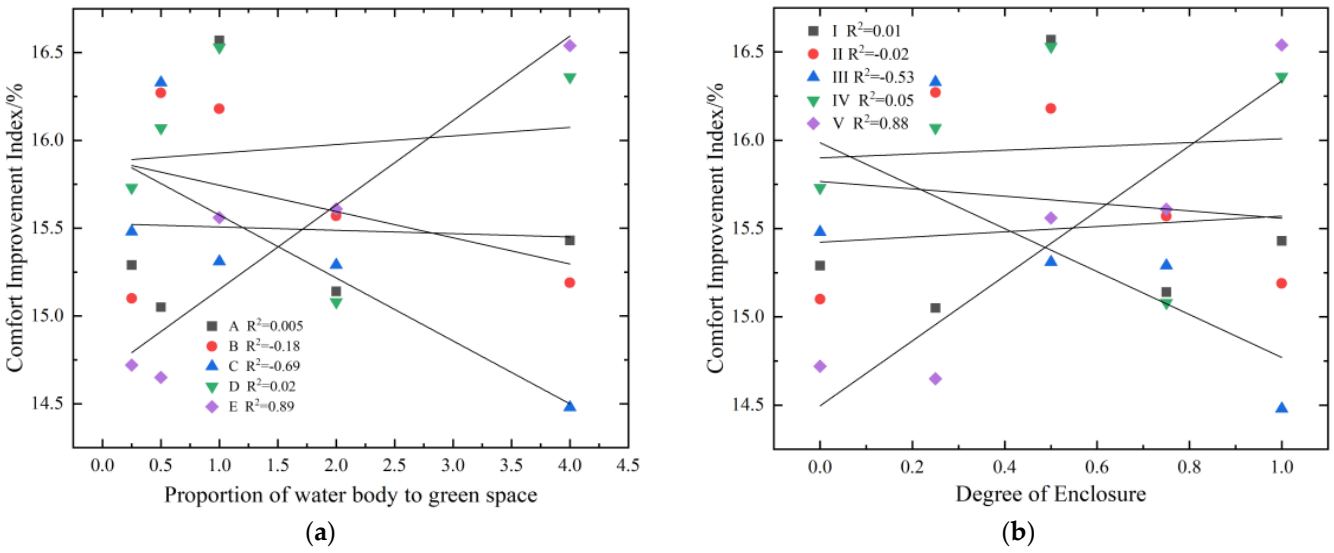


Figure 8. Correlation analysis of enclosure conditions, water body–green space ratio and waterfront space human comfort index. (**a**) Water body–green space ratio; (**b**) Enclosure condition.

Table 7. Waterfront-space human comfort improvement index variation under the effects of different enclosure conditions and waterbody–green space ratios.

Enclosure Condition			Water Body–Green Space Ratio				
Index	**Enclosure Degree**	**Enclosure Direction**	**I-1:4**	**II-1:1.8**	**III-1:1**	**IV-1.8:1**	**V-4:1**
Human comfort improvement index	A	-	15.29	15.10	15.48	15.73	14.72
	B	B1—North	15.03	16.22	16.66	15.61	14.96
		B2—South	15.07	16.34	15.99	16.04	14.98
		B3—West	15.02	16.32	16.45	16.52	14.76
		B4—East	15.06	16.21	16.23	16.11	13.92
	C	C1—West-North	15.90	16.17	15.15	16.02	16.46
		C2—South-North	16.17	16.19	15.38	16.22	15.16
		C3—East-North	17.34	16.61	15.29	17.26	15.15
		C4—West-South	17.38	16.27	15.18	17.27	16.11
		C5—East-West	15.95	15.73	15.43	15.72	15.44
		C6—East-South	16.70	16.10	15.45	16.69	15.05
	D	D1—North-South-West	14.69	14.94	14.71	14.68	15.98
		D2—North-South-East	15.68	16.13	15.94	15.79	15.70
		D3—East-West-North	15.02	15.48	15.27	14.92	16.87
		D4—East-West-South	15.17	15.75	15.24	14.94	13.89
	E	East-South-West-North	15.43	15.19	14.48	16.36	16.54
	Average value		15.68	15.92	15.52	15.99	15.36

4. Discussion

4.1. Microclimatic Effects of Plant Communities in Waterfront Spaces

The analysis of plant microclimate effects in waterfront spaces reveals that the tree–shrub–grass configuration provides the most effective cooling and humidification, surpassing the tree–grass setup. This superior performance is attributed to its more complex vertical layering and pronounced canopy features, characterized by abundant and denser branches and trunks, enhancing heat insulation and moisture retention. These findings align with those of Chang C. et al. [33]. Conversely, grasslands exhibit the least effective cooling and humidification during summer, primarily due to the absence of tall trees like arborvitae, which fail to create a protective shade layer against solar radiation. This observation is consistent with Atsumasa Y.'s research [34]. Additionally, the impact of vegetation spatial structure on wind speed was found to be minimal. However, spaces with a combination of shrubs and grasses showed the most considerable influence on wind speed, contrasting with Liu Binyi et al.'s findings [38]. This discrepancy could result from the limited variation in the vertical and horizontal structures of the plant community, leading to a negligible effect on the wind environment and, consequently, insignificant changes in wind speed.

4.2. Microclimatic Effects of Different Enclosure Conditions and Water Body–Green Space Ratios on Waterfront Spaces

(1) Cooling Index. This simulation study explores the relationship between enclosure conditions, the water body–green space ratio, and their combined effects on cooling. It reveals that the cooling index correlates significantly and positively with the enclosure degree at water body–green space ratios of 1:1 and 1.8:1, with weaker correlations observed at other ratios. This phenomenon likely results from the interplay of enclosure degree, water body size, green space area, and other factors [39]. Previous research indicates that urban temperature variations directly relate to subsurface

structure and composition differences [40], as well as to variations in surrounding vegetation coverage and types, which influence green spaces' abilities to regulate thermal energy [41]. Furthermore, each water body–green space ratio possesses a distinct temperature regulation capacity. As the proportion of water bodies increases, the cooling index initially rises, then declines, suggesting an optimal ratio at 1.8:1 for maximizing cooling effects. Notably, a higher water body proportion does not guarantee improved cooling, aligning with Offerle's findings [42]. Additionally, the degree and orientation of enclosure significantly impact the waterfront space's internal environment. An entirely open site, devoid of shade and subject to high temperatures, can regulate its cooling index by enhancing enclosure, such as increasing tall trees and structures' projection area, modifying microclimatic factors like light and wind speed, or adjusting the water body–green space ratio.

(2) Humidification index. There is a correlation between waterfront-space enclosure and humidification index. Under the same enclosure conditions, the larger the water body–green space ratio, the stronger the humidification effect, which is consistent with the findings of Ranhao et al. [43]. The weakest correlation was found when the water body–green space ratio was 1:4, which might be related to the size of the water body area. The large area of the water body means that the water surface has high albedo and evaporation, which can take away part of the heat during air exchange, thus achieving a good cooling and humidifying effect. At the same time, the open water surface increases the exchange with the dominant wind, further increasing the wind speed, which is similar to the research results of Saaroni H and Steeneveld, G. J. [44,45]. In addition, the shading area and enclosure of tall trees, such as street trees and other tall trees, and the regulation of air circulation also affect the humidity change [46], which is consistent with the research results of Zhu et al. [47].

(3) Ventilation index. The ventilation index assesses the impact of various water body–green space ratios under uniform enclosure conditions on ventilation, corroborating existing research that highlights the positive effects of both water bodies and grasslands on the wind environment [48]. Our experiments demonstrate that spaces without enclosures exhibit a superior ventilation effect due to the reduction in wind obstruction as vertical shading decreases. This facilitates increased airflow and wind speeds during summer [49], echoing the observations of Dan Song et al. [50]. Notably, spaces with a water body–green space ratio of 1:4 achieve the highest ventilation index, attributed to the water surface's minor roughness creating wind channels that enhance wind speed and, consequently, natural ventilation. This setup optimally leverages the water's large specific heat capacity and gradual temperature changes to minimize convection and turbulence between the water surface and air, promoting steady wind flow [51].

(4) Human comfort improvement index. Human comfort is mainly affected by the joint influences of temperature, humidity, and wind speed [52]. Under the same enclosure conditions, the water body–green space ratio of the two-sided enclosure space was negatively correlated with the comfort improvement index; this was inconsistent with the findings of Kuang W H et al. [53], which might be related to the single water-body-plate setting in the simulation software. The water body–green space ratio of the fully enclosed space was significantly positively correlated with the comfort improvement index; under conditions with the same water body–green space ratio, the enclosure was significantly positively correlated with the comfort improvement index when the water body–green space ratio was 4:1. This may be due to the use of green trees as the enclosure method in our simulation, and the tall, leafy trees can impede particular air circulation and form a heat insulation layer [54], which makes the external greenery insulate the external hot and high temperatures. The internal water body environment reduces the temperature and increases the humidity, which results in the improvement of the comfort level.

In addition, The robustness and reliability of our study are significantly enhanced by the size and diversity of the dataset [29], which encompasses 80 distinct scenarios

generated using ENVI-met software based on data collected during the summer solstice. This comprehensive approach ensures that our findings are not confined to a limited set of conditions but are applicable to a wide array of urban waterfront settings. Each scenario represents a unique combination of plant enclosures and water to green space ratios, thereby capturing a diverse range of potential waterfront configurations. The extensive dataset not only underscores the thoroughness of our investigation but also bolsters the validity of our conclusions. Consequently, our research lays a strong foundation for the formulation of adaptable guidelines suitable for diverse urban landscapes.

5. Conclusions

This study employs meteorological measurements and numerical simulations to examine the microclimate impacts of waterfront spaces in summer, specifically focusing on how the characteristics of these spaces influence microclimate effects. Key findings include:

(1) Waterfront vegetation contributes to cooling and humidifying the microclimate, with the effectiveness of different plant communities ranked as follows: tree–shrub–grass > tree–grass > shrub–grass > grass. This research also reaffirms ENVI-met software's scientific reliability and practical utility for microclimate studies.
(2) A water body–green space ratio of 1.8:1 achieves the most significant cooling effect. Enclosure conditions positively impact the cooling index at ratios of 1:1 or 1.8:1.
(3) In terms of humidification, a positive correlation exists between the water body–green space ratio and the humidification index, in descending order of effectiveness: 1.8:1 > 4:1 > 1:1 > 1:1.8 > 1:4. Similarly, enclosure methods correlate positively with the humidification index, ranked as: three-sided > four-sided > two-sided > one-sided > no enclosure.
(4) For ventilation, a ratio of 1:4 between water body and green space, under uniform enclosure conditions, inversely affects the humidification index, with larger water body areas enhancing ventilation.
(5) The optimal ratio for improving human comfort is 1.8:1, with negative correlations observed for a 1:1 ratio in minimally enclosed spaces and positive correlations for a 4:1 ratio in fully enclosed spaces.

Future waterfront-space planning should scientifically determine the appropriate water body–green space ratio to optimize local environmental conditions and human comfort. A 1.8:1 ratio is recommended for cooling needs, while ratios of 4:1 and 1:4 can address humidification and ventilation demands, respectively. If adjusting the ratio is challenging, then modifying the space's enclosure by planting can also enhance the microclimate, with three-sided enclosures favoring cooling, fully enclosed spaces benefiting humidification, and open spaces aiding ventilation.

However, this study has limitations, such as potential measurement errors from mobile measurement and manual reading, and the ENVI-met's sensitivity to computer hardware, which may affect accuracy. Furthermore, the research's focus on a campus setting during summer suggests the need for broader investigations across different locations and seasons to enhance the scientific robustness of the findings.

Author Contributions: Conceptualization, H.X., G.Z., and X.L.; data curation, H.X., G.Z., and X.L.; data analysis, H.X. and X.L.; funding acquisition, Y.J.; investigation, H.X., G.Z., and X.L.; methodology, H.X. and G.Z.; project administration, Y.J.; software, H.X. and G.Z.; supervision, Y.J.; writing—original draft, H.X.; writing—review and editing, G.Z. All authors have read and agreed to the published version of the manuscript.

Funding: This study was funded by Funded by the National Nature Science Foundation (No. 51978480)—Community public green space fairness layout optimization faced to life circle spatial performance a case study of Shanghai.

Institutional Review Board Statement: Not applicable.

Informed Consent Statement: Not applicable.

Data Availability Statement: All images in the text were created by the author. The data used to support the findings of this study are available from the corresponding author upon request.

Conflicts of Interest: The authors declare that they have no known competing financial interests or personal relationships that could have influenced the work reported in this paper.

Appendix A

Table A1. Specific dimensions of modeled scenarios for different enclosure conditions, waterbody–green space ratio.

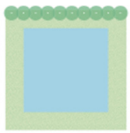
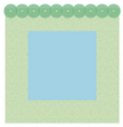
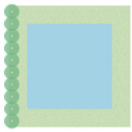
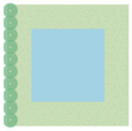
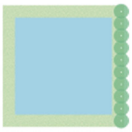
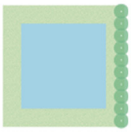
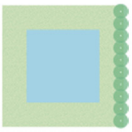
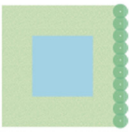
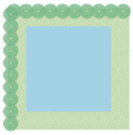
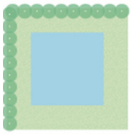
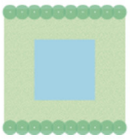
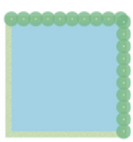
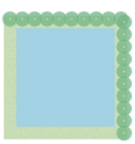
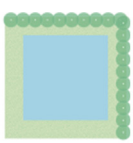
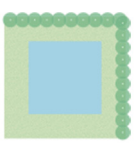
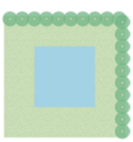
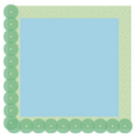
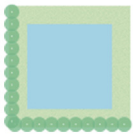
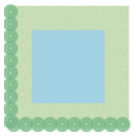
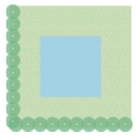
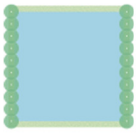
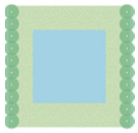
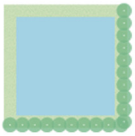
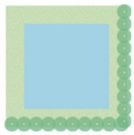
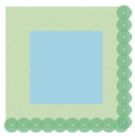
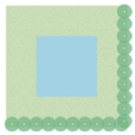
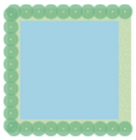
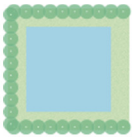
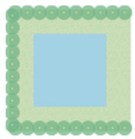
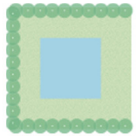
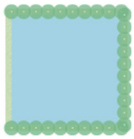
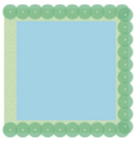
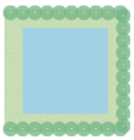
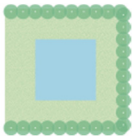
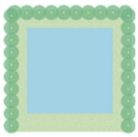
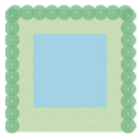
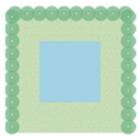
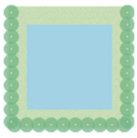
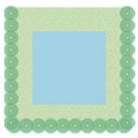
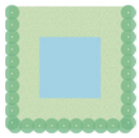
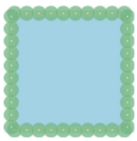
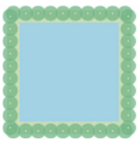
Enclosure Condition		Water Body–Green Space Ratio				
Enclosure Degree	**Enclosure Direction**	**I-1:4**	**II-1:1.8**	**III-1:1**	**IV-1.8:1**	**V-4:1**
A	-					
B	B1—North					
	B2—South					
	B3—West					
	B4—East					
C	C1—West-North					
	C2—South-North					
	C3—East-North					

Table A1. *Cont.*

Enclosure Condition		Water Body–Green Space Ratio				
Enclosure Degree	**Enclosure Direction**	**I-1:4**	**II-1:1.8**	**III-1:1**	**IV-1.8:1**	**V-4:1**
C	C4—West-South					
	C5—East-West					
	C6—East-South					
D	D1—North-South-West					
	D2—North-South-East					
	D3—East-West-North					
	D4—East-West-South					
E	East-South-West-North					

References

1. Morakinyo, T.E.; Lam, Y.F.; Hao, S. Evaluating the role of green infrastructures on near-road pollutant dispersion and removal: Modelling and measurement. *J. Environ. Manag.* **2016**, *182*, 595–605. [CrossRef] [PubMed]
2. Tong, Z. Supporting Information for "Roadside Vegetation Barrier Designs to Mitigate Near-Road Air Pollution Impacts". *Sci. Total Environ.* **2015**, *541*, 920–927. [CrossRef] [PubMed]
3. Hagler, G.S.W.; Lin, M.Y.; Khlystov, A.; Baldauf, R.W.; Isakov, V.; Faircloth, J.; Jackson, L. Field investigation of roadside vegetative and structural barrier impact on near-road ultrafine particle concentrations under a variety of wind conditions. *Sci. Total Environ.* **2012**, *419*, 7–15. [CrossRef] [PubMed]
4. Govindarajulu, D. Urban green space planning for climate adaptation in Indian cities. *Urban Clim.* **2014**, *10*, 35–41. [CrossRef]
5. Fu, B. The Climatic Effects of Waters in Different Natural Conditions. *Acta Geogr. Sin.* **1997**, *52*, 246–253.

6. Aslan, N.; Koc-San, D. Analysis of relationship between urban heat island effect and land use/cover type using Landsat 7 ETM+ and Landsat 8 OLI images. *Int. Arch. Photogramm. Remote Sens. Spat. Inf. Sci.* **2016**, *41*, 821–828. [CrossRef]
7. Li, X.; Ratti, C.; Seiferling, I. Quantifying the shade provision of street trees in urban landscape: A case study in Boston, USA, using Google Street View. *Landsc. Urban Plan.* **2018**, *169*, 81–91. [CrossRef]
8. Morakinyo, T.E.; Kong, L.; Lau, K.L.; Yuan, C.; Ng, E. A study on the impact of shadow-cast and tree species on in-canyon and neighborhood's thermal comfort. *Build. Environ.* **2017**, *115*, 1–17. [CrossRef]
9. Ruhland, C.T.; Day, T.A. Changes in UV-B radiation screening effectiveness with leaf age in *Rhododendron maximum*. *Plant Cell Environ.* **2010**, *19*, 740–746. [CrossRef]
10. Fung, C.K.W.; Jim, C. Influence of blue infrastructure on lawn thermal microclimate in a subtropical green space. *Sustain. Cities Soc.* **2019**, *52*, 101858. [CrossRef]
11. Cheng, S.X.; Jing, L.; Lei, Y. lmpact Analysis of Riverfront Residential Building Design in Northern Region on the Thermal and Humid Environment in Summer. *Build. Sci.* **2015**, *31*, 6.
12. Liu, Z.; Brown, R.D.; Zheng, S.; Jiang, Y.; Zhao, L. An In-Depth Analysis of the Effect of Trees on Human Energy Fluxes. *Urban For. Urban Green.* **2020**, *50*, 126646. [CrossRef]
13. Robitu, M.; Musy, M.; Inard, C.; Groleau, D. Modeling the influence of vegetation and water pond on urban microclimate. *Sol. Energy* **2006**, *80*, 435–447. [CrossRef]
14. Li, K.; Gong, G.; Zou, S. Numerical Simulation of the Impact of Water Body on Building Natural Ventilation. *J. Hunan Univ. (Nat. Sci. Ed.)* **2009**, *36*, 119–123.
15. Xu, X.; Liu, S.; Sun, S.; Zhang, W.; Liu, Y.; Lao, Z.; Guo, G.; Smith, K.; Cui, Y.; Liu, W.; et al. Evaluation of Energy Saving Potential of an Urban Green Space and its Water Bodies. *Energy Build.* **2019**, *188–189*, 58–70. [CrossRef]
16. Jamei, E.; Rajagopalan, P.; Seyedmahmoudian, M.; Jamei, Y. Review on the impact of urban geometry and pedestrian level greening on outdoor thermal comfort. *Renew. Sustain. Energy Rev.* **2016**, *54*, 1002–1017. [CrossRef]
17. Zhao, D.; Lei, Q.; Shi, Y.; Wang, M.; Chen, S.; Shah, K.; Ji, W. Role of Species and Planting Configuration on Transpiration and Microclimate for Urban Trees. *Forests* **2020**, *11*, 825. [CrossRef]
18. Sanusi, R.; Johnstone, D.; May, P.; Livesley, S.J. Microclimate benefits that different street tree species provide to sidewalk pedestrians relate to differences in Plant Area Index. *Landsc. Urban Plan.* **2017**, *157*, 502–511. [CrossRef]
19. Montazeri, H.; Toparlar, Y.; Blocken, B.; Hensen, J. Simulating the cooling effects of water spray systems in urban landscapes: A computational fluid dynamics study in Rotterdam, The Netherlands. *Landsc. Urban Plan.* **2017**, *159*, 85–100. [CrossRef]
20. Jacopo, G.; Kristian, F.; Martina, L. The use of Outdoor Microclimate analysis to support decision making process: Case study of Bufalini square in Cesena. *Sustain. Cities Soc.* **2018**, *42*, 206–215.
21. Marçal, N.A.; da Silva, R.M.; Santos, C.A.G.; dos Santos, J.S. Analysis of the environmental thermal comfort conditions in public squares in the semiarid region of northeastern Brazil. *Build. Environ.* **2019**, *152*, 145–159. [CrossRef]
22. Zakhour, S. The impact of urban geometry on outdoor thermal comfort conditions in hot-arid region. *J. Civ. Eng. Archit. Res.* **2015**, *2*, 862–875.
23. Ketterer, C.; Matzarakis, A. Human-biometeorological assessment of heat stress reduction by replanning measures in Stuttgart, Germany. *Landsc. Urban Plan.* **2014**, *122*, 78–88. [CrossRef]
24. Bruse, M.; Fleer, H. Simulating surface–plant–air interactions inside urban environments with a three dimensional numerical model. *Environ. Model. Softw.* **1998**, *13*, 373–384. [CrossRef]
25. Ziaul, S.; Pal, S. Modeling the effects of green alternative on heat island mitigation of a meso level town, West Bengal, India. *Adv. Space Res.* **2020**, *65*, 1789–1802. [CrossRef]
26. Zhang, L.; Zhan, Q.; Lan, Y. Effects of the tree distribution and species on outdoor environment conditions in a hot summer and cold winter zone: A case study in Wuhan residential quarters. *J. Affect. Disord.* **2018**, *130*, 27–39. [CrossRef]
27. Xu, H.; Zhu, J.; Li, H. Optimization Design of Summer Microclimate Adaptability of Urban Campus Green Space Based on ENVl-met Simulation. *Mod. Urban Res.* **2023**, *38*, 101–106.
28. Emmanuel, R.; Loconsole, A. Green infrastructure as an adaptation approach to tackling urban overheating in the Glasgow Clyde Valley Region, UK. *Landsc. Urban Plan.* **2015**, *138*, 71–86. [CrossRef]
29. Ebrahimabadi, S.; Johansson, C.; Rizzo, A.; Nilsson, K. Microclimate assessment method for urban design—A case study in subarctic climate. *Urban Des. Int.* **2018**, *23*, 116–131. [CrossRef]
30. Oke, T. The urban energy balance. *Prog. Phys. Geogr. Earth Environ.* **1988**, *12*, 471–508. [CrossRef]
31. Wang, Y. Study on Leaf Area Index Characteristics and Influencing Factors of Main Tree Species in Urban Park Green Space of Fuzhou City. Master's, Thesis, Fujian Agriculture and Forestry University, Fuzhou, China, 2018.
32. Xu, H.; Lin, X.; Lin, Y.; Zheng, G.; Dong, J.; Wang, M. Study on the microclimate effect of water body layout factors on campus squares. *Int. J. Environ. Res. Public Health* **2022**, *19*, 14846. [CrossRef]
33. Li, Y.; Song, Y. Optimization of vegetation arrangement to improve microclimate and thermal comfort in an urban park. *Int. Rev. Spat. Plan. Sustain. Dev.* **2019**, *7*, 18–30. [CrossRef]
34. Dui, W.; Xuejiao, D. Environmental meteorology and special weather forecast. *Guangdong Meteorol.* **2000**, *26*, 3–5.
35. Zhang, B.; Amani-Beni, M.; Shi, Y.; Xie, G. The summer microclimate of green spaces in Beijing Olympic Park and their effects on human comfort index. *Ecol. Sci.* **2018**, *37*, 10.

36. Chang, C.R.; Li, M.H.; Chang, S.D. A preliminary study on the local cool-island intensity of Taipei city parks. *Landsc. Urban Plan.* **2007**, *80*, 386–395. [CrossRef]
37. Yoshida, A.; Kinoshita, S.; Hashida, S. Effect of tree canopies on thermal environment, thermal sensation and mental state. *Environ. Eng.* **2013**, *110*, 46a. [CrossRef]
38. Liu, B.Y.; Lin, J. Study on Relationship between Microclimate and Space Section of Urban Waterfront Green Belt A Case Study of Riverfront Green Belt in Suzhou and Shanghai. *Landsc. Archit.* **2015**, *6*, 46–54.
39. Tan, C.L.; Wong, N.H.; Tan, P.Y.; Jusuf, S.K.; Chiam, Z.Q. Impact of plant evapotranspiration rate and shrub albedo on temperature reduction in the tropical outdoor environment. *J. Affect. Disord.* **2015**, *94*, 206–217. [CrossRef]
40. Bowler, D.E.; Buyung-Ali, L.; Knight, T.M.; Pullin, A.S. Urban greening to cool towns and cities: A systematic review of the empirical evidence. *Landsc. Urban Plan.* **2010**, *97*, 147–155. [CrossRef]
41. Song, J.; Wang, Z.-H. Impacts of mesic and xeric urban vegetation on outdoor thermal comfort and microclimate in Phoenix, AZ. *J. Affect. Disord.* **2015**, *94*, 558–568.
42. Offerle, B.; Eliasson, I.; Grimmond, C.S.B.; Holmer, B. Surface heating in relation to air temperature, wind and turbulence in an urban street canyon. *Bound.-Layer Meteorol.* **2007**, *122*, 273–292. [CrossRef]
43. Sun, R.; Chen, A.; Chen, L.; Lü, Y. Cooling effects of wetlands in an urban region: The case of Beijing. *Ecol. Indic.* **2012**, *20*, 57–64. [CrossRef]
44. Saaroni, H.; Ziv, B. The impact of a small lake on heat stress in a Mediterranean urban park: The case of Tel Aviv, Israel. *Int. J. Biometeorol.* **2003**, *47*, 156–165. [CrossRef] [PubMed]
45. Steeneveld, G.; Koopmans, S.; Heusinkveld, B.; Theeuwes, N. Refreshing the role of open water surfaces on mitigating the maximum urban heat island effect. *Landsc. Urban Plan.* **2014**, *121*, 92–96. [CrossRef]
46. Shahmohamadi, P.; Che-Ani, A.I.; Maulud, K.N.A.; Tawil, N.M.; Abdullah, N.A.G. The impact of anthropogenic heat on formation of urban heat island and energy consumption balance. *Urban Stud. Res.* **2011**, *2011*, 497524. [CrossRef]
47. Zhu, X.; Wang, X.; Yan, D.; Liu, Z.; Zhou, Y. Analysis of remotely-sensed ecological indexes' influence on urban thermal environment dynamic using an integrated ecological index: A case study of Xi'an, China. *Int. J. Remote Sens.* **2019**, *40*, 3421–3447. [CrossRef]
48. Hong, B.; Lin, B. Study on Optimal Design of Vegetation in Residential District in Winter Coupling Field Experiment and Numerical Simulation. *Chin. Landsc. Archit.* **2014**, *30*, 104–108.
49. Du, H.; Song, X.; Jiang, H.; Kan, Z.; Wang, Z.; Cai, Y. Research on the cooling island effects of water body: A case study of Shanghai, China. *Ecol. Indic.* **2016**, *67*, 31–38. [CrossRef]
50. Song, D.; Zhang, X.; Zhou, X.; Shi, X.; Jin, X. Influences of wind direction on the cooling effects of mountain vegetation in urban area. *J. Affect. Disord.* **2022**, *209*, 108663. [CrossRef]
51. Tan, Z.; Lau, K.K.-L.; Ng, E. Urban tree design approaches for mitigating daytime urban heat island effects in a high-density urban environment. *Energy Build.* **2016**, *114*, 265–274. [CrossRef]
52. Zhou, X.; Zhang, S.; Zhu, D. Impact of urban water networks on microclimate and PM2. 5 distribution in downtown areas: A case study of Wuhan. *J. Affect. Disord.* **2021**, *203*, 108073.
53. Kuang, W. Seasonal variation in air temperature and relative humidity on building areas and in green spaces in Beijing, China. *Chin. Geogr. Sci.* **2020**, *30*, 75–88. [CrossRef]
54. Muyiti, T.; Han, L.-X.; Jin, J. Numerical simulation of the effects of residual chlorine in cooling water discharge from a power plant on the water environment. *J. Hohai Univ. Nat. Sci.* **2008**, *36*, 475–478.

Disclaimer/Publisher's Note: The statements, opinions and data contained in all publications are solely those of the individual author(s) and contributor(s) and not of MDPI and/or the editor(s). MDPI and/or the editor(s) disclaim responsibility for any injury to people or property resulting from any ideas, methods, instructions or products referred to in the content.